



Contents lists available at ScienceDirect



Applied Catalysis A: General

journal homepage: www.elsevier.com/locate/apcata

The promoting effect of cerium on the characteristics and catalytic performance of palladium supported on alumina pillared clays for the combustion of propene

A. Aznárez, S.A. Korili, A. Gil*

Department of Applied Chemistry, Building Los Acebos, Public University of Navarra, Campus of Arrosadia, E-31006 Pamplona, Spain

ARTICLE INFO

Article history:

Received 22 February 2013

Received in revised form 28 August 2013

Accepted 29 August 2013

Available online xxx

Keywords:

Pillared clays

Palladium supported catalysts

Propene/propylene combustion

Cerium promoting effect

ABSTRACT

The aim of this work was to study the effect of the presence of various amounts of cerium on palladium supported on an alumina pillared clay for the catalytic oxidation of propene. For this purpose, a montmorillonite clay was intercalated and pillared with alumina, then used as a support for palladium. The palladium loading was selected on the basis of previous findings from our group. Cerium loadings of between 0 and 1 wt.% were added after the incorporation of palladium onto the support. The resulting catalysts were characterized by nitrogen physisorption at -196°C , X-ray powder diffraction (XRD), temperature-programmed reduction (TPR) and X-ray photoelectron spectroscopy (XPS). The results obtained suggest that the added Ce partially blocks the microporous volume of the metal catalyst and interacts with the Pd to form new metallic species that enhance the behavior of the initial catalyst in the oxidation of propene.

© 2013 Elsevier B.V. All rights reserved.

1. Introduction

The increasing demand for green energy and the coming into force of more stringent regulations regarding exhaust emissions have been the driving force behind much of the recent research into catalytic combustion technologies. The benefits of catalytic combustion with respect to its traditional thermal counterpart are well established and consist mainly in the formation of lower amounts of by-products due to the lower operating temperatures and higher efficiency [1]. In this respect, although noble metal-based catalysts are well-known for their high performance in the catalytic combustion of hydrocarbons, several studies have investigated the possibility of enhancing the performance of supported noble metal catalysts by adding suitable promoters [2,3].

Pillared Intercalated Clays (PILCs) are an interesting class of two-dimensional microporous materials that can be prepared by the intercalation of inorganic or organic compounds between the silicate layers of clay minerals, which results in an increased basal spacing, pore volume and specific surface area. Due to their textural properties and acidity characteristics, these solid materials are very attractive for adsorption and catalytic applications [4]. Unfortunately, PILCs are not sufficiently stable and tend to collapse, with a resulting loss of textural properties and catalytic performance, at

high temperatures. As such, the thermal stability of the pillars must be increased to avoid the sintering of pillared clays. One way to achieve this goal is to introduce mixed-oxide pillars, such as Al–Ga, Al–Si, Al–Zr, Al–Fe, and Al–Cu, amongst others [5]. Another appropriate way to overcome this problem is to add a rare earth metal. Thus, Sterte [6] found that the incorporation of lanthanide elements during preparation of the intercalating agent resulted in materials whose basal spacing was greater than that of conventional materials. Likewise, an improvement in the thermal stability of Al-pillared clays was reported by Tokarz and Shabtai [7], who prepared pillared clay catalysts by first exchanging the clay with Ce^{3+} or La^{3+} , then exchanging these clays with refluxed, partly hydrolysed Al(III) solutions. The addition of a rare earth metal improves both the thermal stability and the adsorptive and catalytic properties of the pillared materials. CeO_2 has been reported to be able to store and liberate oxygen as a result of the redox properties of the $\text{Ce}^{3+}/\text{Ce}^{4+}$ pair, which can result in good performance for the combustion of Volatile Organic Compounds (VOCs). Supported palladium catalyst is known to be effective for the combustion of VOCs and many research works investigate the possibility of enhancing the catalytic activity by using CeO_2 as suitable support or adding this oxide as promoter to the supports. The properties of the supports are modified by the presence of CeO_2 . Farrauto et al. [8] reported a beneficial effect of the presence of CeO_2 as support on the stabilization of PdO . The effect of CeO_2 addition to alumina-support is studied by various authors [9–13] on supported catalysts for the methane combustion. Similarly, various authors have reported that the presence of Ce in Pd/Al-pillared clays produces a substantial decrease in the

* Corresponding author. Tel.: +34 948 169602; fax: +34 948 169602.

E-mail address: andoni@unav.es (A. Gil).

temperature required for the complete oxidation of benzene [14,15]. In all these studies the properties of the supports are modified and after wet impregnation with a palladium solution, new catalysts are obtained. In the present work, various amounts of cerium are added to a supported palladium catalyst and the characteristics and catalytic performance on the combustion of propene studied. The catalyst was selected from a previous work [16] considering the possibility of modification of the catalytic behavior by the presence of a promoter.

2. Experimental

2.1. Catalyst preparation

The starting material was a montmorillonite from Tsukinuno, supplied by the Clay Science Society of Japan. The raw clay was pillared with alumina according to a conventional pillarizing procedure [17], then used as catalytic support. The supported palladium catalyst was prepared by wet impregnation of the support with a solution of palladium ($\text{Pd}(\text{NO}_3)_2$, palladium(II) nitrate solution, 10 wt.% in 10 wt.% HNO_3 , Sigma-Aldrich) to obtain a material with a metal loading of 0.1 wt.%. The metal salt/clay slurry was evaporated under reduced pressure in a rotavapor and the resulting solid dried at 120 °C for 16 h before being calcined in air at 500 °C for 4 h to form the final supported catalyst. The modified catalysts were prepared by treating 5 g of the Pd catalyst with 50 cm³ of aqueous $\text{Ce}(\text{NO}_3)_3 \cdot 6\text{H}_2\text{O}$ solutions (99.99%, Sigma-Aldrich) to obtain loadings of between 0 and 1 wt.%. The metal salt/catalyst slurries were evaporated under reduced pressure in a rotavapor and the resulting solids dried at 120 °C for 16 h before being calcined in air at 500 °C for 4 h to form the final modified catalysts. The catalytic series are referred to as wt. CePd, where wt. indicates the cerium content.

2.2. Catalyst characterization

Nitrogen adsorption experiments (Air Liquide, 99.999%) at –196 °C were performed using a static volumetric apparatus (Micromeritics ASAP 2010 adsorption analyser). All samples (0.2 g) were degassed for 24 h at 200 °C at a pressure lower than 0.133 Pa. The Langmuir surface area (S_{Lang}) was calculated from nitrogen adsorption data over the relative pressure range 0.01–0.05, considering a nitrogen molecule cross-sectional area [18] of 0.162 nm². The total pore volume (V_p) was estimated from the amount of nitrogen adsorbed at a relative pressure of 0.99, assuming that the density of the nitrogen condensed in the pores is equal to that of liquid nitrogen at –196 °C (0.81 g/cm³) [18]. The micropore volumes ($V_{\mu p}$) were calculated using the Dubinin–Radushkevich equation [19] over the relative pressure range 0.01–0.034.

After extraction by acid digestion, the metal contents were determined by inductively coupled plasma optical emission spectroscopy (ICP-OES) using a Varian Vista-MPX instrument. X-ray diffraction (XRD) patterns of nonoriented powder samples were obtained using a Siemens D-5000 diffractometer fitted with a Ni-filtered Cu K α radiation source, at 40 kV and 30 mA. Temperature-programmed reduction (TPR) studies were carried out using a Micromeritics TPR/TPD 2900 instrument. An initial pre-treatment with N_2 (Air Liquide, 99.999%) was carried out at 150 °C for 90 min, at a heating rate of 10 °C/min, under a flow of 30 cm³/min, to condition the samples. TPR tests were then carried out from room temperature up to 800 °C, at a heating rate of 10 °C/min, under a total flow of 30 cm³/min (5% H_2 in Ar, Air Liquide). Water and other compounds that might be formed during metal reduction and precursor decomposition were retained by a molecular sieve trap. Hydrogen consumption was measured using a thermal conductivity detector (TCD).

X-ray photoelectron spectroscopy (XPS) analyses were performed using an SSI X-probe (SSX-100/206) spectrometer from Surface Science Instruments (USA). The analysis chamber was operated under ultrahigh vacuum at a pressure close to 5×10^{-7} Pa, and the sample was irradiated with monochromatic Al K α (1486.6 eV) radiation (10 kV; 22 mA). Charge compensation was achieved using an electron flood gun adjusted to 8 eV and placing a nickel grid 3.0 mm above the sample. The pass energy for the analyzer was set at 150 eV for both wide and narrow scans, and an area of approximately 1.4 mm² was analyzed. Under these conditions, the full width at half-maximum (fwhm) of the Ag 3d_{5/2} peak from a silver standard sample was about 1.6 eV. For these measurements, the binding energy (BE) values were referred to the C-(C,H) contribution of the C 1s peak at 284.8 eV. Data treatment was performed using the CasaXPS program (Casa Software Ltd., UK), and some spectra were deconvoluted using the least squares fitting routine incorporated in this software with a Gaussian/Lorentzian (85/15) product function and after subtraction of a non-linear baseline. Molar fractions were calculated using peak areas normalized on the basis of acquisition parameters and sensitivity factors provided by the manufacturer. The C 1s, O 1s, Mg 2s, Si 2p, Al 2p, Ce 3d and Pd 3d peaks were used for quantitative analysis. Based on the XPS analysis, the XPS surface ratio of a given element is defined as the atomic concentration of the element (%) with respect to the concentration of the major element of the support (Si) (%).

2.3. Catalytic performance

Propene combustion was carried out using an automated bench-scale catalytic unit (Microactivity Reference, PID Eng & Tech). The reactor was a tubular, fixed-bed, downflow type with an internal diameter of 0.9 cm. Catalyst samples were mixed with an inert material, at a weight ratio of 1:4, in order to dilute the catalyst bed and avoid hot spot formation. The propene concentration in the feed was 0.5% and the oxygen-to-hydrocarbon molar ratio was 20, with helium as the balance gas, up to a total feed flow of 150 cm³/min. The catalyst was stabilized for 120 min at each temperature to ensure steady-state conversion. Space velocities (GHSV), calculated at standard temperature and pressure and based on the volume of the catalytic bed, were about 20,000 h⁻¹. Prior to the catalytic tests, one of the following pre-treatments were applied to the catalysts: (1) in flowing air (100 cm³/min): heating to 150 °C at 2 °C/min, 2 h at 150 °C and cooling to room temperature, or (2) in flowing H_2 (Air Liquide, 99.999%) (100 cm³/min): heating to 300 °C at 2 °C/min, 2 h at 300 °C and cooling to room temperature. The reactant and reaction product streams were analyzed online using an Agilent 6890 gas chromatograph system.

3. Results and discussion

The most important differences between the nitrogen adsorption isotherms of the samples are found at relative pressures lower than 0.10 (see Fig. 1), in other words in the micropore region. The textural properties of the materials obtained are presented in Table 1. The Al-PILC used as catalytic support in this work shows a specific surface area of 158 m²/g. A comparison of the textural properties of the support, the Pd catalyst and the Ce-modified catalysts showed that the surface and volume accessibilities are affected by the presence of the metals, especially in the case of Ce. The loss of specific surface area caused by the presence of Pd is around 26%, with this value increasing to 53–63% in the presence of Ce. For OCePd as well as for Ce-modified catalysts, the decrease in the microporous surface is much more significant than that in the external surface. These results are attributed to the presence of the smaller particles of palladium on the microporous region

Table 1

Textural properties derived from N₂ adsorption at –196 °C, chemical analyses and temperatures at which the conversion of propene reaches 10% and 90%.

Catalyst	$S_{\text{Lang}}^{\text{a}}$ (m ² /g)	$S_{\mu\text{p}}^{\text{b}}$ (m ² /g)	$S_{\text{ext}}^{\text{c}}$ (m ² /g)	V_p^{d} (cm ³ /g)	$V_{\mu\text{p}}^{\text{e}}$ (cm ³ /g)	Pd (wt.%)	Ce (wt.%)	T_{10}^{f} (°C)	T_{90}^{f} (°C)	T_{10}^{g} (°C)	T_{90}^{g} (°C)
Al-PILC	159	140	19	0.111	0.060	–	–	–	–	–	–
0CePd	117	100	18	0.092	0.044	0.13	0.01	252	326	229	315
0.01CePd	58	44	14	0.063	0.022	0.12	0.03	254	322	234	303
0.1CePd	75	59	17	0.081	0.029	0.12	0.17	–	–	249	306
1CePd	66	53	13	0.066	0.025	0.11	1.64	–	–	254	320

^a Specific surface area calculated using the Langmuir equation.

^b Specific micropore surface area.

^c Specific external surface area obtained from the *t*-plot method.

^d Specific total pore volume.

^e Specific micropore volume derived from the Dubinin-Radushkevich (DR) equation.

^f Temperatures after pre-treatment in air.

^g Temperatures after pre-treatment in hydrogen.

and of the bigger ones on the external surface. The cerium phase is mainly situated on the external surface, blocking the entrance to the micropores, and in interaction with the palladium bigger particles, as confirmed by the TPR analysis. These results could be explaining if the impregnation aqueous solution of cerium can produce the dissolution of the palladium with a new reorganization of the metal on the surface of the Al-PILC.

The XRD patterns for the supported palladium and Ce-modified catalysts are presented in Fig. 2. The fact that patterns for these samples did not reveal the presence of PdO or Pd⁰ could be related to the low loading of this metal and its high dispersion on the

support. As far as the crystalline phases of Ce are concerned, diffraction peaks at 28.6° ((1 1 1), $I = 100\%$), 33.2° ((2 0 0), $I = 30\%$), 47.5° ((2 2 0), $I = 52\%$) and 56.4° ((3 1 1), $I = 42\%$) (JCPDS file no. 34-0394) were only detected for the 1CePd catalyst and correspond to CeO₂ oxide. No peaks resulting from other Ce species, or for the 0.01CePd and 0.1CePd catalysts, were detected. This could also be related to the low Ce content.

The TPR profiles for the catalysts are presented in Fig. 3. In the case of the 0CePd catalyst, the first region of H₂ consumption, which is observed between 100 and 200 °C, is attributed to the reduction of small PdO species (oxide clusters). The subsequent reduction process in the temperature range of 200–460 °C is attributed to the reduction of bigger PdO particles that interact strongly with the surface of the support [20]. The significant reduction process observed at 640 °C was assigned to the reduction of structural Fe³⁺ cations of the support. It should also be noted that the reduction processes at temperatures higher than 550 °C can be ascribed to reduction and thermal decomposition of the sample (thermogravimetric analysis does not form part of this work). In agreement with the above, a similar reduction process was observed for the CePd catalysts at between 100 and 200 °C. As in the case of the Pd catalyst, for the catalysts 0.01CePd and 0.1CePd this process is due to the reduction of small PdO particles. In the case of 1CePd, however, the reduction process that commences at 100 °C is much more pronounced than those observed for the other catalysts, probably due to the reduction of small PdO particles interacting with the cerium oxide. The reduction maximum in the temperature range 200–460 °C shifted to higher temperatures for all the Ce-modified catalysts. Various authors have related the presence of a maximum at 360 °C to the reduction of non-stoichiometric Ce oxides [12,13]. Thus, the addition of varying amounts of Ce to the catalyst results in an interaction between the Ce and both large PdO particles and the

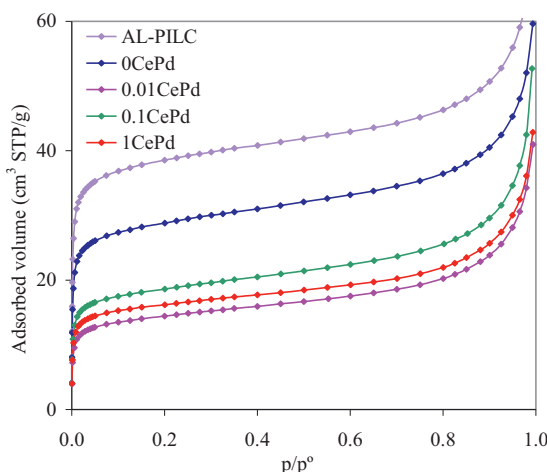


Fig. 1. Nitrogen adsorption isotherms for the CePd catalysts at 196 °C.

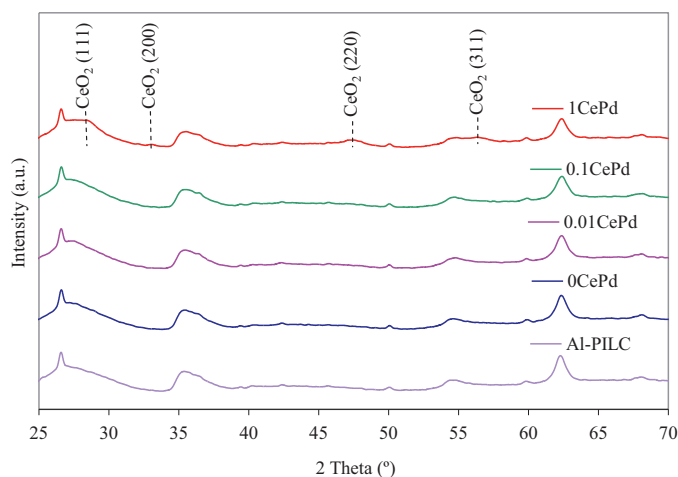


Fig. 2. XRD patterns for the CePd catalysts calcined in air at 500 °C for 4 h.

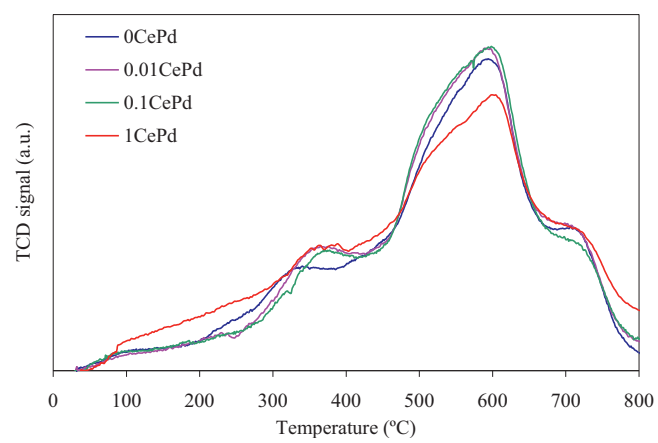


Fig. 3. TPR patterns for the CePd catalysts.

Table 2

Binding Energies (BEs) and atomic ratios obtained from XPS experiments.

Catalyst	Binding energies (eV)					Atomic Surface Ratio			
	O 1s	Si 2p	Mg 2s	Al 2p	Pd 3d _{5/2}	Ce/Si	O/Si	Pd/Si	Al/Si
Al-PILC	532.0	102.9	89.5	74.9	—	—	3.11	—	0.60
0CePd	532.1	103.0	89.6	75	338.1	336.5	—	3.51	0.0011
0.01CePd	532.1	103.0	89.6	75	338.1	336.5	335.1	0.0023	0.61
0.1CePd	532.1	103.0	89.6	75	338.1	336.5	—	0.0052	0.60
1CePd	532.1	103.0	89.6	75	338.1	336.5	—	0.0176	0.62

support, resulting in the formation of non-stoichiometric Ce oxides, which are reduced at 360–380 °C. The reducibility of the bigger PdO particles is diminished by the presence of these oxides.

The binding energies (BEs) and atomic ratios of the catalysts, as determined by XPS, are presented in **Table 2**. Typical BEs for montmorillonite are 102.75 (Si 2p_{3/2}), 74.8 (Al 2p_{3/2}) and 532 eV (O 1s) [21]. The addition of Pd, followed by Ce, did not result in significant changes to the BEs of the principal elements in the support. The XPS results also show that all the catalysts, with the same Pd loading but different cerium loading, have the same surface atomic Pd/Si ratio. Pd-Ce interaction contributes, as it has been previously reported [22], to either palladium redispersion or maintenance of a highly dispersed state. A comparison of the ratio between surface and total Ce (from chemical analysis, see **Table 1**) gives the following order with respect to Ce amount: 0.074 (0.01CePd)>0.030 (0.1CePd)>0.011 (1CePd). As a result, it can be concluded that, in accordance with the nitrogen adsorption results, the amount of Ce that penetrates the structure of the support during synthesis increases with Ce content. The O/Si ratio suggests that cerium addition increases the presence of oxygen on the surface. Deconvolution of the XPS spectra of the catalysts into their individual components showed that there were three forms of palladium present on the surface. The BEs measured for the Pd 3d_{5/2} line, which are in accordance with those reported in the literature, were 335.1, 336.5 and 338.1 eV. The BE at 335.1 eV can be attributed to Pd⁰, and that at 336.5 eV, which is comparable to an oxidized palladium foil standard (336.7 eV), was attributed to bulk PdO. The peak at 338.1 eV was attributed to highly dispersed and sufficiently coordinated Pd²⁺ in contact with the support to form palladium-aluminate structures. Thus, the XPS results show that at low surface concentrations oxidized palladium exists in two chemical states, namely bulk PdO and palladium-support structures. The percentage of the chemical states of palladium and cerium (Ce³⁺/Ce⁴⁺) in the surface of the catalysts is presented in **Table 3**. For 0CePd the percentage of bulk PdO (70%) is considerably higher than that of palladium-support structures (30%). In the case of the Ce-modified catalysts, the percentage of palladium-support structures increases (50–85%) while the percentage of bulk PdO decreases (10–50%), with respect to 0CePd catalyst, which is related to the Pd/Ce/support interaction. On increasing the metal loading from 0.1%wt. to 1%wt. it is shown that the percentage of Ce³⁺ decreases while that of Ce⁴⁺ increases. The higher cerium loading in 1CePd leads to a bigger CeO₂ crystallite size, as shown by XRD analysis. In line with these results, the lower percentage of palladium-support structures in 1CePd (50%) with regard to 0.01CePd (85%) and 0.1CePd (90%) is explained also in terms of a bigger CeO₂

crystallite size, which leads to lower Pd/Ce/support interaction. Monteiro et al. [22], who studied the role of the Pd precursors in the oxidation of CO over Pd/Al₂O₃ and Pd/CeO₂/Al₂O₃ catalysts, concluded that Pd-Ce interaction was promoted by ceria species in its reduced state (Ce³⁺). Thus, in the lower-loaded Ce catalysts (0.01CePd and 0.1CePd) the interaction Pd/Ce/support and the percentage of reduced ceria (Ce³⁺) are higher than in the higher-loaded ones (1CePd).

The conversion of propene over the 0CePd catalyst after various pre-treatments in flowing air or hydrogen is shown in **Fig. 4A**. The catalytic conversion was calculated in terms of propene consumption and CO₂ formation. The values obtained were compared and found to be generally in good agreement. Furthermore, our results show that the complete oxidation of propene depends on the pre-treatment of the 0CePd catalyst only slightly, being the catalytic performance of the catalyst slightly improved by the pre-treatment in flowing hydrogen. Various authors [9–11] also described that the presence of CeO₂ does not significantly affect catalytic performances in the combustion of methane, but markedly affects high temperature catalytic behavior in line with the stabilization of active PdO species. To ensure a better comparison, the T₁₀ and T₉₀ values (temperatures at which propene conversion reaches 10% and 90%, respectively) are included in **Table 1**. After treatment of the catalyst at 300 °C, some of the noble metal oxide, even that which interacts strongly with the support, is reduced (see **Fig. 3**). Thus, the catalytic effect is due to the fact that reduction of the oxides, and thus formation of the active phase in the reaction (Pd⁰), occurs during the reductive pre-treatment.

The effect of the presence of Ce on the catalytic behavior is presented in **Fig. 4B–D**. In **Fig. 4B** it is shown a decrease in the catalytic activity of the 1CePd catalyst, in respect of the 0CePd sample, when a reductive pre-treatment at 300 °C is applied. It is explained due to its bigger CeO₂ crystallite size, which leads to lower Pd/Ce/support interaction, and thus to a smaller catalytic activity. An improvement of the activity for 0.01CePd and 0.1CePd catalysts, in comparison with the 0CePd catalyst, is observed for high temperatures, approximately from 300 °C. The high activity of the pre-reduced samples is discussed in terms of reduction of CeO₂ in the vicinity of the metal particles [23,24], and a decreasing CeO₂ crystallite size that leads to higher metal/Ce interaction and hence greater activity [25]. Monteiro et al. [22] pointed out a cause in not observing hydrocarbon oxidation at low temperatures. They concluded that during CO oxidation at low temperatures, oxygen uptake went directly to replenish the ceria oxygen-deficient lattice, instead of oxidizing CO. There would then be a fierce competition between the CeO_x species and Pd sites by the molecule

Table 3

Palladium and cerium surface composition (%) obtained from XPS experiments.

Catalyst	BEs (EV)–Pd 3d _{5/2}			Oxidized palladium	Reduced Palladium	Ce ³⁺	Ce ⁴⁺
	338.1 (Pdn _{n≥2})	336.5 (Bulk PdO)	335.1 (Pd ⁰)				
0CePd	30	70	—	100	—	—	—
0.01CePd	85	10	5	95	5	—	—
0.1CePd	90	10	—	100	—	51	49
1CePd	50	50	—	100	—	41	59

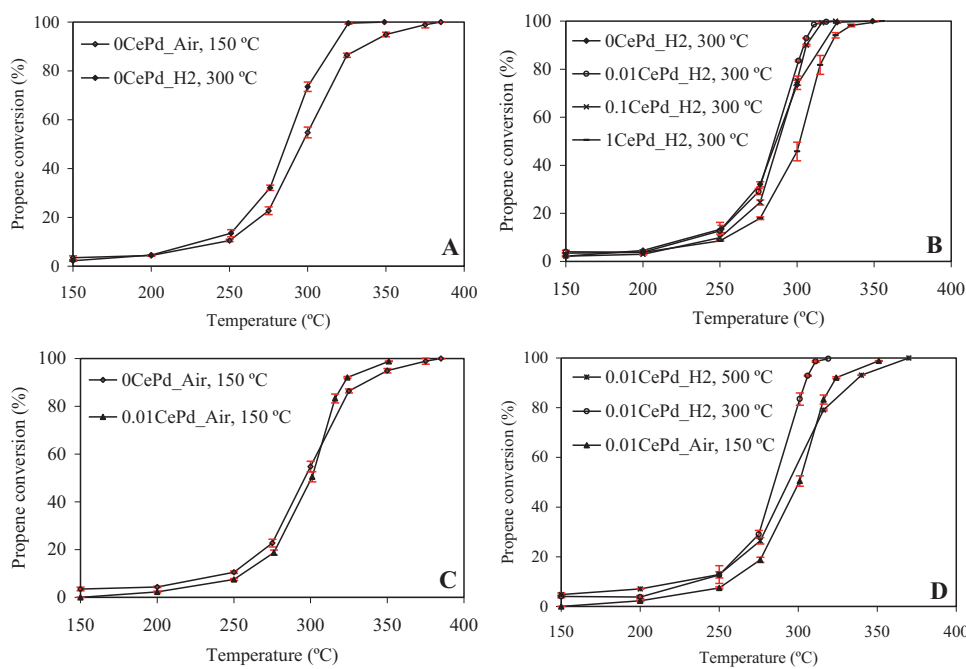


Fig. 4. Conversion of propene over palladium and palladium-cerium modified catalysts after air and hydrogen pre-treatments.

of oxygen. Thus, oxygen would be available to CO oxidation only after complete re-oxidation of ceria reduced species. Ceria reduced species (Ce^{3+}) were not able to help CO to oxidize due to lack of oxygen in its lattice. Hence, the highest rates of CO oxidation were only observed at higher temperatures as a result of strong competition for oxygen molecules. Unfortunately, this enhancement disappeared with an oxidative pre-treatment and in lean conditions, and the reactivity was similar to that of 0CePd, see Fig. 4C. It has been reported that in these conditions, the active sites of the interface Pd/Ce/support and Pt/Ce/support are converted into an oxidized and less active state, disappearing the promoter effect of ceria [24]. The effect of the pre-treatment with hydrogen at 500 °C is shown in Fig. 4D, being observed a decrease in the catalytic activity of the 0.01CePd catalyst pre-treated in hydrogen at 500 °C when compared to that pre-treated in hydrogen at 300 °C. Several authors [23,26] have reported that reduction of a noble metal/ceria catalyst at high temperature, above 500 °C, induced some kind of strong metal-support interaction (SMSI) effect, decreasing the catalytic activity of the sample. Keeping in mind that, as pointed out by nitrogen adsorption, Ce partially blocks the microporous region, meaning that those palladium species do not take part in propene combustion, it is important to note the high activity of the palladium/cerium/support interface. As such, the Pd particles affected by the presence of Ce must be sufficiently active to support the catalytic performance of the initial catalyst, or improve it from 300 °C when they are pre-reduced in hydrogen at 300 °C.

4. Conclusions

It is concluded that a reduction pre-treatment at 300 °C resulted in a higher activity than a reduction pre-treatment at 500 °C, or an oxidative pre-treatment at 150 °C. The Ce loading plays a key role, as when big CeO_2 crystallites are formed, a lower Pd/Ce/support interaction and thus a smaller catalytic activity are observed.

Acknowledgements

This work was funded by the Spanish Ministry of Science and Innovation (MICINN) and the European Regional Development Fund (FEDER) (project MAT2007-66439-C02). The authors would

like to thank P. Eloy, *Université catholique de Louvain* (Belgium), for XPS measurements. A. Aznárez acknowledges financial support from the Public University of Navarra through a PhD fellowship.

References

- [1] R.L. Garten, R.A. Balla Betta, J.C. Schlatter, Catalytic combustion, in: G. Ertl, H. Knözinger, J. Weitkamp (Eds.), *Handbook of Heterogeneous Catalysis*, vol. 4, Wiley-VCH: Einheim, Germany, 1997, p. 1668.
- [2] A. Ishikawa, S. Komai, A. Satsuma, T. Hattori, Y. Murakami, *Appl. Catal. A General* 110 (1994) 61–66.
- [3] W. Hua, Z. Gao, *Appl. Catal. B Environ.* 17 (1998) 37–42.
- [4] A. Gil, S.A. Korili, R. Trujillano, M.A. Vicente, *Pillared Clays and Related Catalysts*, Springer Science, New York, 2010.
- [5] A. Gil, M.A. Vicente, L.M. Gandia, *Catal. Rev.-Sci. Eng.* 42 (2000) 145–212.
- [6] J. Sterte, *Clays Clay Miner.* 39 (1991) 167–173.
- [7] M. Tokarz, J. Shabtai, *Clays Clay Miner.* 33 (1985) 89–98.
- [8] R.J. Farrauto, J.K. Lampert, M.C. Hobson, E.M. Waterman, *Appl. Catal. B Environ.* 6 (1995) 263–270.
- [9] G. Groppi, C. Cristiani, L. Lietti, C. Ramella, M. Valentini, P. Forzatti, *Catal. Today* 50 (1999) 399–412.
- [10] P.O. Thevenin, A. Alcalde, L.J. Pettersson, S.G. Järas, J.L.G. Fierro, *J. Catal.* 215 (2003) 78–86.
- [11] S. Colussi, C. de Leitenburg, G. Dolcetti, A. Trovarelli, *J. Alloys Compd.* 374 (2004) 387–392.
- [12] R. Ramirez-Lopez, I. Elizalde-Martinez, L. Balderas-Tapia, *Catal. Today* 150 (2010) 358–362.
- [13] L.S.F. Feio, C.E. Hor, S. Damyanova, F.B. Noronha, W.H. Cassinelli, C.M.P. Marques, J.M.C. Bueno, *Appl. Catal. A Gen.* 316 (2007) 107–116.
- [14] S.H. Zuo, Q. Huang, R. Zhou, *Catal. Today* 139 (2008) 88–93.
- [15] S.H. Zuo, R. Zhou, *Microporous Mesoporous Mater.* 113 (2008) 472–480.
- [16] A. Aznárez, F.C.C. Assis, A. Gil, S.A. Korili, *Catal. Today* 176 (2011) 328–330.
- [17] A. Gil, R. Trujillano, M.A. Vicente, S.A. Korili, *Adsorpt. Sci. Technol.* 25 (2007) 217–226.
- [18] S.J. Gregg, K.S.W. Sing, *Adsorption, Surface Area and Porosity*, Academic Press, New York, 1991.
- [19] M.M. Dubinin, *Carbon* 27 (1989) 457–467.
- [20] A.S. Ivanova, E.M. Slavinskaya, R.V. Gulyaev, V.I. Zaikovskii, O.A. Stonkus, I.G. Danilova, L.M. Plyasova, I.A. Polukhina, A.I. Boronin, *Appl. Catal. B Environ.* 97 (2010) 57–71.
- [21] S. Barama, C. Dupeyrat-Batiot, M. Capron, E. Bordes-Richard, O. Bakhti-Mohammed, *Catal. Today* 141 (2009) 385–392.
- [22] R.S. Monteiro, L.C. Dieguez, M. Schmal, *Catal. Today* 65 (2001) 77–89.
- [23] A. Holmgren, F. Azarnoush, E. Fridell, *Appl. Catal. B Environ.* 22 (1999) 49–61.
- [24] C. Serre, F. Garin, G. Belot, G. Maire, *J. Catal.* 141 (1993) 9–20.
- [25] J.G. Nunan, H.J. Robot, M.J. Cohn, S.A. Bradley, in: A. Crucp (Ed.), *Catalysis and Automotive Pollution Control II*, Elsevier, Amsterdam, 1991, pp. 221–227.
- [26] S.E. Golunski, H.A. Hatcher, R.R. Rajaram, T.J. Trux, *Appl. Catal. B Environ.* 5 (1995) 367–376.